Improved spectral resolution in time-varying interferometry

Julián Antonacci [a,*], Eneas N. Morel [b], Jorge R. Torga [b], Ricardo Duchowicz [c,d], Gustavo F. Arenas [a]

[a] Instituto de Investigaciones Científicas y Tecnológicas en Electrónica (ICyTE), Facultad de Ingeniería, Universidad Nacional de Mar del Plata, Juan B. Justo 4302, Mar del Plata, Argentina & CONICET, Argentina.
[b] Laboratorio de Optoelectrónica y Metrología Aplicada, Facultad Regional Delta, UTN, San Martin 1771,(2804), Campana, Buenos Aires, Argentina & CONICET, Argentina.
[c] Centro de Investigaciones Ópticas (CONICET-CIC), Centenario y 506, Gonnet, La Plata, Argentina
[d] Universidad Nacional de la Plata, Facultad de Ingeniería, Calle 1 1900, La Plata, Argentina

ABSTRACT

In this work, we present a procedure that allows increasing the resolution of dynamic length measurements made by spectral interferometry. The proposed scheme leads to obtaining a compact photonic instrument with the ability to measure distances, variations on positions and vibrations with a very high resolution. This measurement system includes a superluminescent source (SLED), a digital spectrometer and a Fizeau interferometer. Spectral data is processed by applying Fourier domain techniques previously applied in optical coherence tomography. The resolution of the spectral measurement system is determined by the spectrometer bandwidth and the light source employed. A signal is obtained by analysing the time evolution of a single pixel from the spectrometer CCD sensor, which is later analysed using time domain interferometry (TDI) techniques. This procedure works by detecting changes in the optical path below those that can be detected by spectral analysis. The original resolution obtained with the solely spectral techniques was 2.2 μm but was improved to 40 nm by complementary analysis of temporal signals.

1. Introduction

Fibre optic sensors are very attractive due to their sensitivity characteristics, non-invasively and electrical noise immunity [1,2] and on top, they have the capability of being multiplexed two or more sensors in the same system [3,4]. They are useful for measurements within the volume of the samples as in thickness measurements of paints and coatings [5]. Conventional mechanical sensors can damage or deform the analysed surface leading to inaccurate measurements.

The development of optical communications has made fibre optic sensors accessible by providing components that allow the design of complex devices with high sensitivity and resolution. These sensors besides being potentially used in conventional applications are particularly useful where traditional techniques do not offer solutions [6]. Some years ago, we focused our attention on an extrinsic distance sensor based on a Fizeau interferometer. This sensor does not require calibration and is contact-free with the surface being studied. Also, it includes all the known common goodness of interferometric fibre optics sensors [3,7].

The Fizeau interferometer (FI) used as a time domain interferometry (TDI) instrument is implemented with a laser as a source and a power detector. TDI has become a very precise technique for the measurement of distances variations in the cases where the direction of the displacement is not a variable to be determined, and this was demonstrated

in previous work in the determination of contraction of dental resins [8] and the characterisation of polymer vitrification [9].

Although TDI does not provide absolute information about the cavity length, it is a very attractive technique because of its high resolution and low cost. On the other hand, spectral domain interferometry (SDI) could lead to absolute value measurements with the same Fizeau interferometer using a broadband source and a spectrometer instead of a LASER and a power detector.

Recently, in previous work, we presented the possibility to simultaneously measure the same length [10] using the same measurement system, without moving parts, for two different interferometric techniques (SDI and TDI). The signals from both techniques were obtained from the same interferometer having their sources and detectors decoupled in wavelength. TDI does not provide absolute information of the cavity length but can give information of the variations in this length with greater resolution than the spectral technique. Then, better results are obtained by combining both techniques (TDI + SDI) than with each one.

Following this path, in this work we present a substantial advance on the system design, reducing the number of components, leading to higher light efficiency, improving the resolution of length variations measurements and reducing the system cost. It is reached measuring absolute lengths using the SDI, improving the measurement resolution of length variations by TDI but without adding couplers, a laser and a
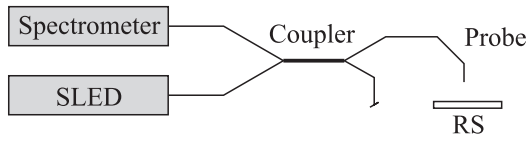
Fig. 1. Fibre optic Fizeau interferometer. RS: Refractive surface.

detector as used in reference [10], leading to a higher light efficiency and reducing the system price. The system is constituted by a single interferometer without moving parts using a single broadband light source and a spectrometer. The TDI signal can be obtained following the power measured by a single pixel of the spectrometer.

The dynamic range of TDI depends on the coherence length of the laser in [10]. If the laser source spectral density is assumed to be Gaussian, the coherence length is directly proportional to $\lambda_0^2/\Delta\lambda$ being λ_0 the central wavelength and $\Delta\lambda$ the wideband [1]. By applying this technique, the degradation of interferograms visibility depends on the bandwidth of a spectrometer pixel instead of the source, increasing the dynamic range remarkably.

It is possible to achieve several interferograms from the same measurement simply by choosing as individual pixels as required. It also can be useful to avoid the ambiguity when a cavity sense change occurs at interferogram maxima or minima. A study of the range of applicability of this method is also performed.

2. Materials and methods

The Fizeau interferometer considering two different detection schemes, TDI and SDI, are described as follows:

The fibre optic Fizeau interferometer scheme is depicted in Fig. 1. In this type of instrument, the light reflected at the end of the pigtail interferes with the light reflected on the surface under analysis. A detailed study of the device can be found in reference [10] and [11].

Here, a SLED broadband light emitter operating at 800 nm with a normalised spectral distribution $S(\lambda)$ is employed as a light source, where λ is the spectral wavelength. The unilateral power spectral density at the output of the interferometer is given by Eq. 1 [10]

$$G(\lambda) = G_0 \cdot S(\lambda)\left[1 + \frac{2\sqrt{R_1 R_2}\beta}{R_1 + \beta R_2(1 - R_1)^2} \cdot \cos\left(\frac{4\pi n_0 d}{\lambda}\right)\right] \quad (1)$$

where G_0 is the mean power spectral density, n_0 is the cavity refraction index, and d is the cavity length to be determined. R_1 and R_2 are the reflectivities at the end of the fibre and the surface to be measured, respectively. The β parameter is the cavity length dependence and can be calculated as:

$$\beta = [1 + 2 \cdot Ad/(2\pi)]^{-1} \quad (2)$$

Eq. (2) is obtained from the axial loss for single-mode (SM) fibres, with $A = \lambda \cdot \ln(V)/R_2$, where V is the effective frequency of the fibre ($V \leq 2.404$ for SM fibres).

a. Fourier Transform-Spectral Domain Interference (FD-SDI)

Changing the variable λ by defining $u = 2/\lambda$, Eq. (1) can be expressed as:

$$G(u) = G_0 S(u)\left[1 + \frac{2\sqrt{R_1 R_2}\beta}{R_1 + \beta R_2(1 - R_1)^2} \cdot \cos(2\pi \cdot d \cdot u)\right] \quad (3)$$

Although β has a λ dependence, it changes much slower than the cosine of $4\pi n_0 d/\lambda$ [8]. Eq. (3) shows two spectrally separated components, both modulated by $G_0 S(u)$. $G(u)$ have one constant term and a second term which frequency is d.

Therefore, the value to be obtained (d) is found as the frequency of a sinusoid modulated by the curve of the spectral density of the source. Filtering can remove the low-frequency component. Different types of techniques have been developed to obtain d from Eq. (3). A comparison
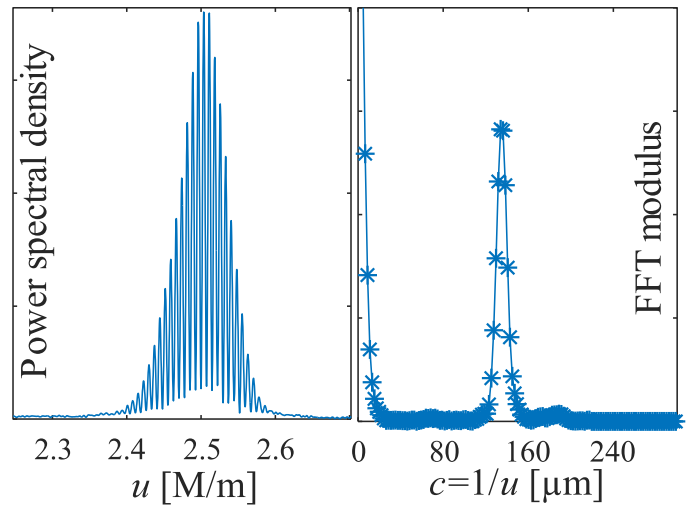

Fig. 2. Spectrum for a 135 μm cavity and its FFT.

between the use of the Fourier Transform (FT) and the iterative phase-lock method can be found in reference [12]. Also, a technique based on the use of fuzzy inference systems was developed in reference [13].

The FT of $G(u)$ from u domain to the $c = 1/u$ domain can be defined as $D(c) = F\{G(u)\}$. Based on the linearity of the FT we can distribute the relation as follows:

$$D(c) = F\{G_0 S(u)\} + F\left\{G_0 S(u)\frac{2\sqrt{R_1 R_2}\beta}{R_1 + \beta R_2(1 - R_1)^2}\cos(2\pi \cdot d \cdot u)\right\} \quad (4)$$

Finally, using the product properties in the untransformed domain and knowing that the unilateral FT of $\cos(2\pi du)$ is $\delta(c-d)$ then $D(c)$ can be written:

$$D(c) = F\{G_o S(u)\} + F\left\{G_o S(u)\frac{2\sqrt{R_1 R_2}\beta}{R_1 + \beta R_2(1 - R_1)^2}\right\} \otimes \delta(c - d) \quad (5)$$

where the "$\otimes$" operator represents the convolution product.

The FT is defined for a continuous function, for discrete functions the discrete Fourier transform (DFT) must be used. In this work, the DFT is computed by the fast Fourier transform (FFT) algorithm [14].

A typical spectrum regarding u, obtained from a cavity of 135 μm, can be seen in Fig. 2 (left), while in Fig. 2 (right), the amplitude of its FFT is shown. It is possible to easily discriminate the low-value components of c and those convolved with $\delta(c-d)$. The d value of the cavity can be obtained as the location in c of the peak in the amplitude of $D(c)$. In this case, the value is 134 μm. The difference between the measured value and the real value is that the FFT has equally-spaced points, where each $\Delta c = 1/AB_u$, and AB_u is the bandwidth of the measurement regarding u. If it is expressed as a function of the wavelength, we can obtain the resolution of the d measurement:

$$\Delta c = (u_{max} - u_{min})^{-1} = \left(\frac{2}{\lambda_{min}} - \frac{2}{\lambda_{max}}\right)^{-1} = \frac{1}{2}\cdot\left(\frac{1}{\lambda_{min}} - \frac{1}{\lambda_{max}}\right)^{-1} \quad (6)$$

Defining λ_{min} and λ_{max} as the minimum and maximum wavelength of the spectrometer and not the source, for the spectrometer used ($\lambda_{min} = 740$ nm and $\lambda_{max} = 890$ nm), $\Delta c \approx 2.2$ μm.

b. Time domain Interference (TDI) analysis

The TDI signal is generated following the power value from a pixel of the spectrometer as a function of time. The pixel acts as an optical power sensor in which the received intensity depends on the detection bandwidth of the spectrometer´s pixel ($\Delta\lambda$) and the central wavelength of the pixel λ_0. The bandwidth detected by the pixel is determined by dividing the bandwidth of the spectrometer by the total number of pixels. Then, the detected intensity is given by the integral of Eq. (1) within

the bandwidth of the pixel:

$$I(\lambda_0, d) = \int_{\lambda_0 - \Delta\lambda/2}^{\lambda_0 - \Delta\lambda/2} G(\lambda) \cdot d\lambda = I_0(\lambda_0)\left[1 + \gamma \cos\left(\frac{2\pi}{\lambda_0} \cdot 2 \cdot d\right)\right]$$

$$\gamma = \frac{2\sqrt{R_1 R_2 \beta}}{R_1 + \beta R_2(1-R_1)^2} \qquad (7)$$

$$I_0(\lambda_0) = \int_{\lambda_0 - \Delta\lambda/2}^{\lambda_0 - \Delta\lambda/2} G_0 \cdot S(\lambda) \cdot d\lambda$$

As shown in Eq. (7), the term in square brackets is taken as a constant over the pixel bandwidth. The spectral distribution acts as an envelope that varies slowly with wavelength.

If we consider d as a time function $d = d(t)$ we can obtain the intensity $I(t)$ as:

$$I(t) = I_0 + I_0 \cdot \gamma \cdot \cos\left[\frac{2\pi}{\lambda_0} \cdot 2 \cdot d(t)\right] \qquad (8)$$

The wavelength associated with the pixel under study is λ_0 and γ is the fringe visibility. By filtering, the static term (I_0) can be separated from the dynamic one ($I_f(t)$). Therefore:

$$I_f(t) = I_0 \cdot \gamma \cdot \cos\left[\frac{2\pi}{\lambda_0} \cdot 2 \cdot d(t)\right] \qquad (9)$$

Eq. (9) shows the function that we must analyse to obtain $d(t)$ when it varies with time. Because the signal is obtained by a spectral analyser which has a limited sampling frequency, it is important to study the bandwidth of $I_f(t)$ to determine the applicability of this method.

Assuming that the cavity is subjected to a sinusoidal vibration, with an A_d amplitude, an oscillation frequency f_d and an average value of d_0, we can describe its dynamics as:

$$d(t) = d_0 + A_d \cos(2\pi \cdot f_d \cdot t) \qquad (10)$$

By replacing Eq. (10) in Eq. (9) we can obtain:

$$I_f(t) = I_0 \cdot \gamma \cdot \cos\left[\frac{4\pi \cdot d_0}{\lambda_0} + \frac{4\pi \cdot A_d}{\lambda_0} \cdot \cos(2\pi \cdot f_d \cdot t)\right] \qquad (11)$$

The cosine of the sum in Eq. (11) could be expanded as a product of sines and cosines and can be written as a summation of sinusoids with frequencies that are multiples of f_d:

$$I_f(t) = I_0 \cdot \gamma \cdot \sum_{n=-\infty}^{\infty} J_n(\kappa) \cos[2\pi(n f_d)t + \kappa \cdot d_0/A_d] \qquad (12)$$

where $\kappa = 4\pi A_d/\lambda_0$. In Eq. (12), $J_n(\kappa)$ is the Bessel coefficient of the first species of order n and parameter κ.

According to Eq. (12), $I_f(t)$ has components across the frequency spectrum but since the Bessel coefficients decrease in magnitude rapidly from certain values of n, a range of coefficients of importance can be determined, and the remainders neglected. Fig. 3 shows the amplitudes of the Bessel coefficients for three different κ values where we can notice the dependence on the number of coefficients.

The number of significant coefficients that produce a relevant proportion of the energy on the signal is finite, and the number of coefficients of interest depends on κ. In particular, 98% of the signal energy is contained if both positive and negative κ coefficients are considered and coincide with half of the bandwidth of a phase modulated (PM) signal according to the Carson criterion since the signal $I_f(t)$ is a typical PM signal but without carrier [15]. Finally, the bandwidth of the signal is approximated as follows:

$$\text{BW} \simeq \kappa \cdot f_d = \frac{4\pi}{\lambda_0} A_d f_d \qquad (13)$$

Fig. 4 shows the relationship between the frequency f_d, the amplitude A_d and the bandwidth generated by the TDI signal.

The minimum sampling frequency required to obtain a one-pixel oscillogram of the spectrum analyser, avoiding the aliasing problem is $f_s > 2\text{BW}$ according to the Nyquist criterion [14,16]. Because the bandwidth obtained in Eq. (13) is approximate, it is suggested to use at least three times the approximate bandwidth. It is evident that the BW of the
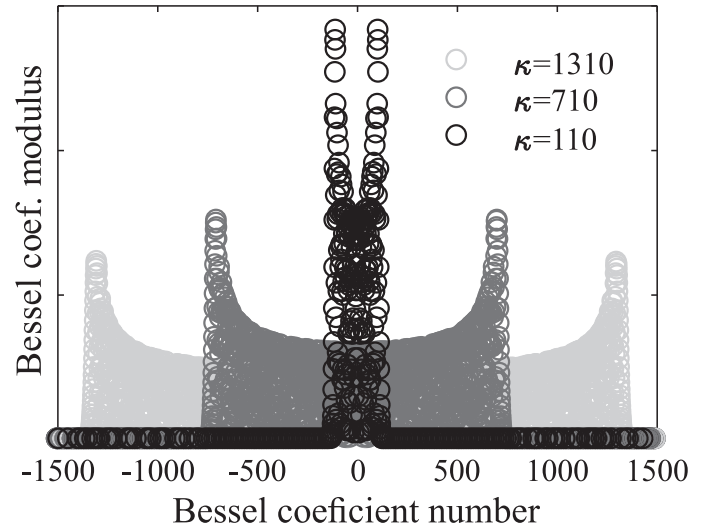

Fig. 3. Modulus of Bessel coefficients for different values of κ: 1310 (light grey), 710 (grey) and 110 (black).
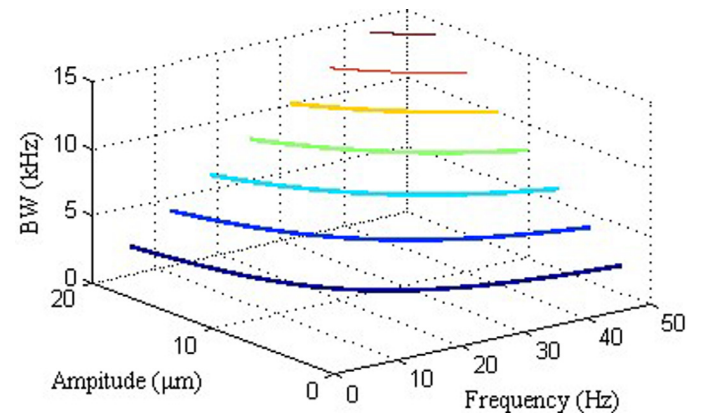

Fig. 4. TDI signal bandwidth as a function of amplitude and frequency of vibration.

TDI signal depends directly on the amplitude and frequency of the cavity variation and for the same frequency value, the amplitude changes the BW and vice versa. If the previous conditions are met, then from the oscillogram the cavity length ($d(t)$) can be obtained. Eq. 9 shows that between maxima of the oscillogram the cavity length changes in $\lambda_0/2$ then, between a maximum and a minimum changes in $\lambda_0/2$. If a cycle of the oscillogram is discretised in ten, then the achieved resolution is $\lambda_0/20$.

3. Results and discussions

The first configuration employed combines two independent interferometers to compare the results obtained using one as a reference and the other as a system under study (Fig. 5). The cavities of both measurement systems have different lengths but vary with the same magnitude in the opposite direction as the length of the piezoelectric actuator (PZT - 6F-607 by Thorlabs) excited with a signal at 100 mHz using a Thorlabs MDT694 *driver* and a Hewlett Packard 33120A signal generator. The reference sensor is the same used in multiple applications [17–19] with a laser centred at 1310 nm as an optical source, a 50:50 (2×2) coupler and a Thorlabs DET410 detector.

The proposed sensor light source used was a superluminescent LED (SLED) centred at 800 nm with 40 nm bandwidth. An Ocean Optics HR4000 spectral analyser was used. The 50:50 (2×2) coupler is a Thorlabs 10202A-50. Samples were acquired for 18 s at 10 ksps in the ref-
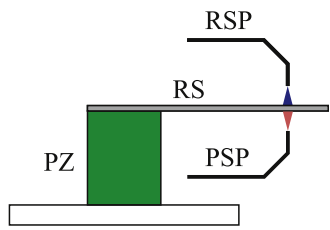
Fig. 5. Measurement system setup. RSP: Reference sensor probe, PSP: Proposed sensor probe, RS: Reflective surface, PZ: Piezoelectric actuator.
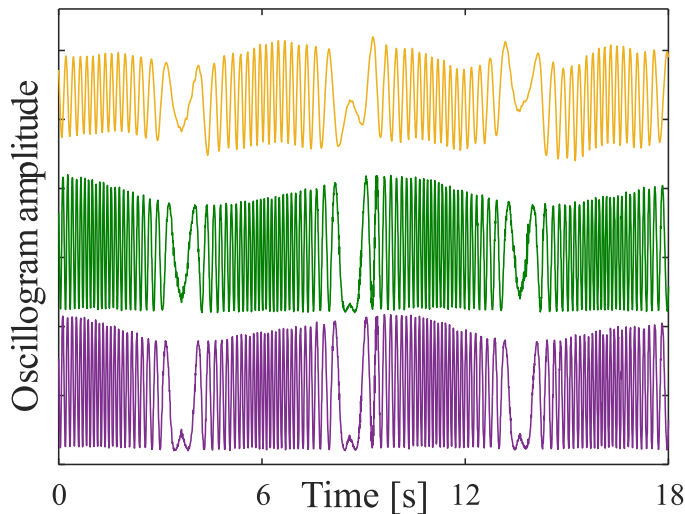

Fig. 6. Oscillograms of the classical TDI method (yellow) and corresponding to two different wavelengths from the spectrum analyser (green and purple). (For interpretation of the references to colour in this figure legend, the reader is referred to the web version of this article.)

Fig. 7. Variation of $d(t)$ for a sinusoidal source obtained by FD-SDI (blue), TDI laser + FD-SDI (red) and TDI + SDI by the proposed method (yellow). (For interpretation of the references to colour in this figure legend, the reader is referred to the web version of this article.)

Fig. 8. Variation of $d(t)$ obtained by FD-SDI (blue) and TDI + FD-SDI by the proposed method (red) for a triangular source. (For interpretation of the references to colour in this figure legend, the reader is referred to the web version of this article.)

erence system and 125 spectra per second in the system under study. Fig. 6 shows the oscillogram corresponding to the reference system and two different spectrometer pixels corresponding to 793.6 and 800.9 nm wavelengths. The oscillogram of the reference system has lower visibility than the oscillogram of the proposed method. Nevertheless is not seen in Fig. 6 because a constant value is added to each oscillogram to improve its visualisation. This difference in the visibility is due to the bandwidth of the laser and the spectrometer's pixel. Typical laser diodes have a linewidth in the order of 1 nm, the spectrometer used in this work has 3648 pixels between 708.05 nm and 892.31 nm (50 pm pixel bandwidth). Then, the $\lambda_0^2/\Delta\lambda$ coefficient is remarkably improved.

Fig. 7 shows the results obtained by the reference system, FD-SDI of the system under test and a TDI signal by the proposed method with the oscillogram of 800.9 nm.

Since TDI curves do not have an absolute length value, it only contains information of relative displacement. A constant value is added to obtain the same mean value than the FD-SDI curve. The direction change of the TDI curves does not come from the measurement itself, but it must be done with the information given by the FD-SDI. This is why the red and yellow curves (Fig. 7) come from both TDI + FD-SDI, rather than from TDI [10].

In a second step, spectra were acquired only with the system showed in Fig. 1 while the PZ actuator was excited with a triangular signal of 100 mHz. The plots resulting from processing the FD-SDI and TDI + FD-SDI are shown in Fig. 8. In this case, the TDI signal was simply obtained by following a pixel of the spectrometer.

Finally, the system was used to characterise the expansion of a thermal microscope plate upon heating. The expansion was measured due to the variation of the cavity length while the temperature was obtained by reading th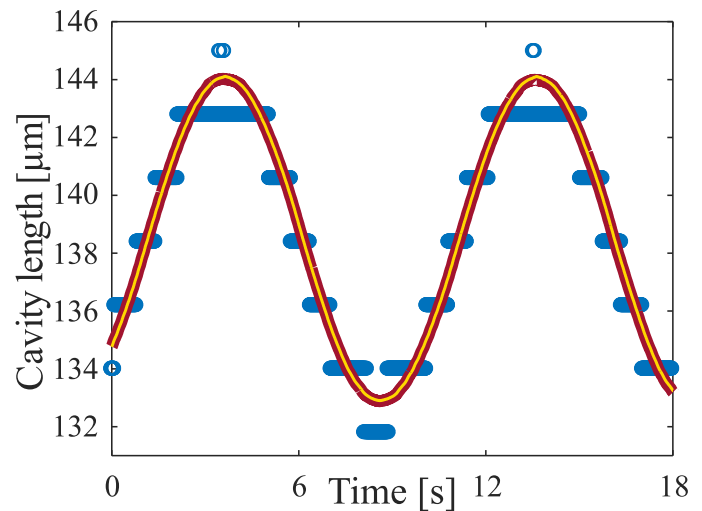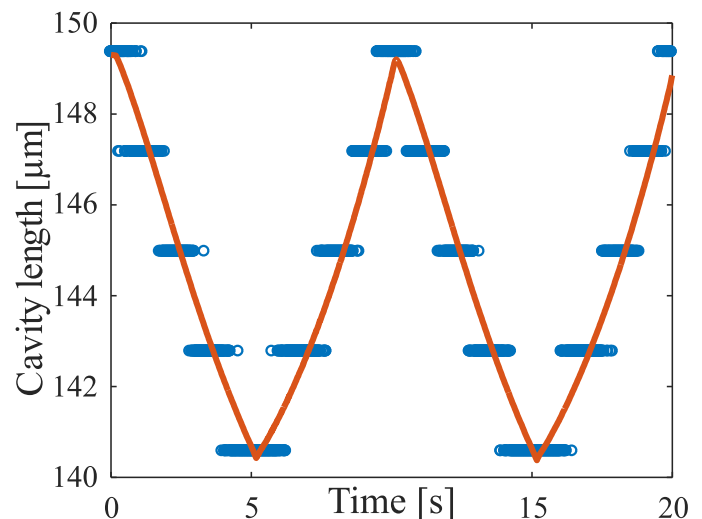e internal platinum sensor (Texas Instruments LM35). The cavity length curves obtained by the FD-SDI and TDI + DF-SDI and the temperature are shown in Fig. 9.

It is important to remark that jumps appear in the FD-SDI reconstructed signals as a system resolution limitation. Using the TDI signal a resolution of 40 nm is achieved.

The length of the cavity as a function of temperature is shown in Fig. 10 where the slope of the line shown is directly related to the thermal expansion coefficient of the material employed to build the thermal microscope plate (Aluminum).

4. Conclusion

A robust system, with no moving parts and completely embedded in optical fibre was presented to measure absolute cavity lengths with the FD-SDI technique, which improves the resolution to approximately the order of a TDI Fizeau interferometer that is tenths of microns. In previous work, it was necessary to deal with complex optical arrangements to obtain similar results, here we achieved them with a simpler scheme.
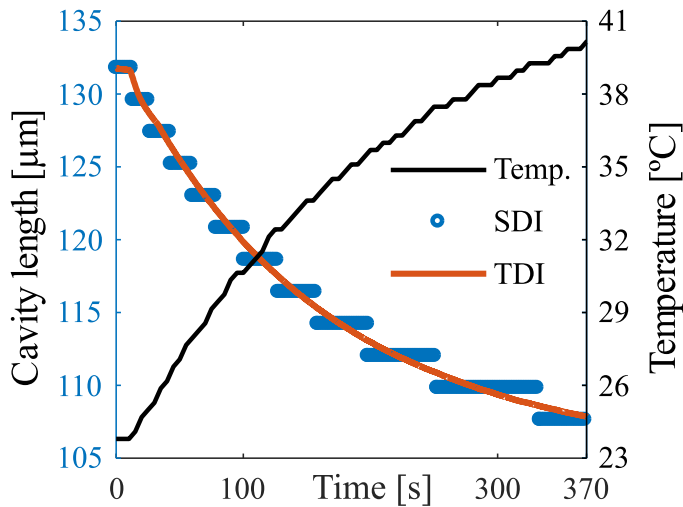
Fig. 9. *d(t)* obtained by FD-SDI, FD-SDI + TDI and temperature.
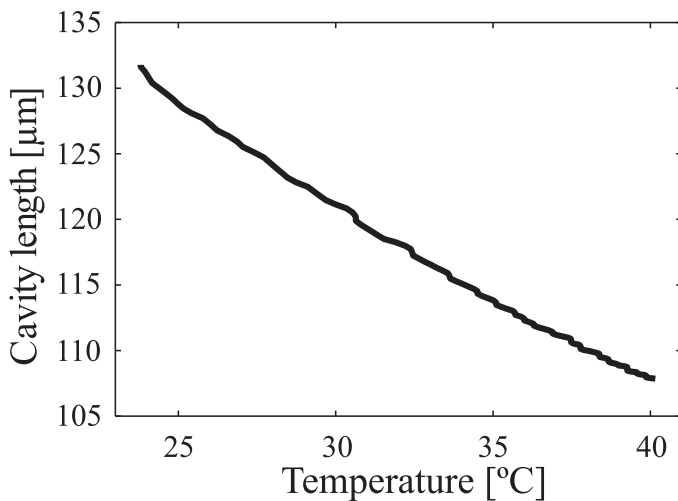

Fig. 10. Expansion vs. Temperature.

Being SDI a spectral sensor, the sample rate is strongly limited by the time integration of the spectrometer. In this sense, a detailed analysis related to the TDI signal bandwidth was obtained for a sinusoidal vibrations case and could be extrapolated to other types of signals as well.

Although the FD-SDI system dynamic range limitations depend on the analyser spectral resolution, a limitation using the spectra to extract the TDI signals lies on the acquisition sampling interval. Care must be taken to avoid this issue, specifically on the acquisition speed.

However, we demonstrate the resolution enhancement of the proposed method to measure signals of low amplitude and low frequency, such as in wide biological phenomena, thermal expansions and big structures vibrations.

5. Funding sources

This work has been supported by: Instituto de Investigaciones Científicas y Tecnológicas en Electrónica (ICyTE), Facultad de Ingeniería,

References

[1] Krohn DA, MacDougall TW, Mendez A. Fiber optic Sensors: fundamentals and applications. Fourth Edition. SPIE PRESS BOOK; 2015.

[2] Yin S, Ruffin PB, Yu FTS. Fiber optic sensors. Second Edition. CRC Press; 2008.

[3] S.M. Musa, R.O. Claus, J.H. Reed, R.L. Simpson, A. Wang, K.A. Murphy, J. Reed, R. Simpson, Real-time signal processing and hardware development for a wavelength modulated optical fiber sensor system, 1997.

[4] Rao YJ, Jiang J, Zhou CX. Spatial-frequency multiplexed fiber-optic Fizeau strain sensor system with optical amplification. Sens Actuators A 2005;120:354–9.

[5] Morel EN, Torga JR. Dynamic detection of thicknesses in polymer deformation based on the optical coherence interferometry technique.. Bentham Science Publishers LTD. Open Phys J 2015;2:6.

[6] Udd E. Fiber optics sensors – an introduction for engineers and scientists. USA: John Wiley & Sons; 1991. p. 274–7.

[7] Udd E. Fiber optic sensors. Boston, USA: SPIE; 1992.

[8] Arenas GF, Noriega S, Vallo C, Duchowicz R. Polymerization shrinkage of a dental resin composite determined by a fiber optic Fizeau interferometer. Opt Commun 2007;271:581–6.

[9] Arenas GF, Duchowicz R. Vitrification of photo-curing resins by embedded cantilever and Fizeau interferometer. In: Proceedings of SPIE, the international society for optical engineering; 2011. p. 8011.

[10] Antonacci J, Arenas GF, Duchowicz R. Double domain wavelength multiplexed Fizeau interferometer with high resolution dynamic sensing and absolute length detection. Opt Lasers Eng 2017;91:227–31.

[11] A.M. Mesa Yandy, G.F. Arenas, J. Antonacci, S. Noriega, R. Duchowicz, Analysis of temporal and spectral response of an optical fiber Fizeau interferometer applied to the study of photocurable resins, 2015 XVI Workshop on Information Processing and Control (RPIC), pp. 1–5.

[12] Gurov I, Hlubina P, Chugunov V. Evaluation of spectral modulated interferograms using a Fourier transform and the iterative phase-locked loop method. Meas Sci Technol 2003;14:122.

[13] Antonacci J, Meschino GJ, Passoni LI, Arenas GF. Spectral Fizeau Interferometer spectra processing by means of a fuzzy inference system. In: 2015 XVI Workshop on Information Processing and Control (RPIC); 2015. p. 1–6.

[14] Oppenheim AV, Schafer RW, John RB. Discrete-time signal processing. New Jersey: Printice Hall Inc; 1989.

[15] Carlson AB, Crilly PB. Communication Systems: an introduction to signals and noise in electrical communication. 5 ed. McGraw-Hill; 2010.

[16] Rabiner LR, Gold B. Theory and application of digital signal processing, 777. Englewood Cliffs, NJ: Prentice-Hall, Inc.; 1975. p. 1.

[17] Arenas GF, Duchowicz R. Measurements of the solidification process of resins from cantilever beams resonances. Opt Commun 2013;286:140–5.

[18] Arenas GF, Noriega S, Claudia VI, Duchowicz R. Polymerization shrinkage of a dental resin composite determined by a fiber optic Fizeau interferometer. Opt. Commun. 2007;271:581–6.

[19] Arenas GF, Noriega S, Mucci V, Claudia VI, D R. Contraction Measurements of Dental Composite Material during Photopolymerization by a Fiber Optic Interferometric Method. AIP Conf. Proc. 2008;992:225–30.